New Phytologist
Research

Mistletoes have higher hydraulic safety but lower efficiency in xylem traits than their hosts

Yun-Bing Zhang[1], **Xian-Yan Huang**[1,2], **Marina Corrêa Scalon**[3], **Yan Ke**[1,4], **Jing-Xin Liu**[1], **Qin Wang**[1,4], **Wen-Hua Li**[1], **Da Yang**[1], **David S. Ellsworth**[5], **Yong-Jiang Zhang**[6,7] and **Jiao-Lin Zhang**[1]

[1]CAS Key Laboratory of Tropical Forest Ecology, Xishuangbanna Tropical Botanical Garden, Chinese Academy of Sciences, Menglun, Mengla, 666303, Yunnan, China; [2]School of Ecology and Environmental Science, Yunnan University, Kunming, 650500, China; [3]Programa de Pós-graduação em Ecologia e Conservação, Universidade Federal do Paraná, Curitiba, PR, 81531-990, Brazil; [4]University of Chinese Academy of Sciences, Beijing, 100049, China; [5]Hawkesbury Institute for the Environment, Western Sydney University, Locked Bag 1797, Penrith, NSW, 2751, Australia; [6]School of Biology and Ecology, University of Maine, Orono, ME 04469, USA; [7]Climate Change Institute, University of Maine, Orono, ME 04469, USA

Authors for correspondence:
Jiao-Lin Zhang
Email: zhangjiaolin@xtbg.ac.cn

Yong-Jiang Zhang
Email: yongjiang.zhang@maine.edu

Received: *28 July 2024*
Accepted: *22 October 2024*

New Phytologist (2024)
doi: 10.1111/nph.20257

Key words: conservative water use strategy, hemiparasitic plants, host quality hypothesis, hydraulic architecture, trade-off between hydraulic efficiency and safety.

Summary

- Both mistletoes and their hosts are challenged by increasing drought, highlighting the necessity of understanding their comparative hydraulic properties. The high transpiration of mistletoes requires efficient water transport, while high xylem tensions demand strong embolism resistance, representing a hydraulic paradox.
- This study, conducted across four environments with different aridity indices in Yunnan, China, examined the xylem traits of 119 mistletoe–host species pairs.
- Mistletoes showed lower water use efficiency, indicating a more aggressive water use. They also showed lower hydraulic efficiency (lower vessel diameter and theoretical hydraulic conductivity) but higher safety (lower vulnerability index and higher conduit wall reinforcement, vessel grouping index, and wood density) compared with their hosts, supporting the trade-off between efficiency and safety. Environmental variation across sites significantly affected xylem trait comparisons between mistletoes and hosts. Additionally, the xylem traits of mistletoes were strongly influenced by host water supply efficiency. The overall xylem trait relationships in mistletoes and hosts were different.
- These findings stress the impact of host and site on the hydraulic traits of mistletoes, and suggest that mistletoes may achieve high transpiration by maintaining high stomatal conductance under low water potentials. This study illuminates the distinctive adaptation strategies of mistletoes due to their parasitic lifestyle.

Introduction

Mistletoes are an important component of the ecosystem as keystone species and ecosystem engineers, impacting various ecosystem processes and ecosystem responses to climate change (Watson & Herring, 2012; Fontúrbel *et al.*, 2018; Bell *et al.*, 2020; Crates *et al.*, 2022; Griebel *et al.*, 2022; Watson *et al.*, 2022). However, their differential hydraulic traits and hydraulic strategies, in comparison with their hosts, remain poorly understood. Mistletoes, resembling small shrubs due to their short stature, are hemiparasitic plants that obtain water and nutrients directly from their hosts via specialized haustoria, distinguishing them from epiphytes (Glatzel & Geils, 2009). This parasitic nature makes the hydraulic pathlength longer than their individual lengths, and thus, the height and hydraulics of the hosts need to be considered in studying their hydraulic traits and pathways (Fajardo, 2022). Since they are located at the canopy of their hosts, mistletoes must endure relatively lower leaf water potentials than their hosts (He *et al.*, 2021; Ye *et al.*, 2021) and they typically maintain higher stomatal conductance and transpiration rates (Yang *et al.*, 2017; Zhang *et al.*, 2023) for effective water and nutrient uptake (Glatzel & Geils, 2009). Furthermore, mistletoes encounter a paradoxical challenge in their parasitic lifestyle: while their relatively high stomatal conductance and transpiration rates require efficient water transport, high xylem tensions (low water potentials) demand strong embolism resistance. How mistletoes balance the paradoxical hydraulic demands remains unknown to date, but is important in predicting their responses to increasing drought and transpirational demand driven by rising global temperatures and the associated shifts in climate patterns. As such, this paradox underscores the need to investigate their hydraulic traits and water use strategies.

Hydraulic architecture, vital for plant water transport and drought response, is governed by wood xylem morphological and anatomical traits (Scholz *et al.*, 2013; Tng *et al.*, 2018; Lens *et al.*, 2022). For instance, vessel diameter directly influences hydraulic efficiency according to Hagen-Poiseuille's law, with larger diameters offering greater efficiency but increasing the risk of dysfunction (Tyree & Zimmermann, 2002; Hacke *et al.*, 2022). This hydraulic efficiency and safety trade-off has been proposed to explain the difference in hydraulic strategies among co-occurring species. However, this trade-off is recently under debate as it may be weak or decoupled in some cases, indicating that the relationship is species-specific or dependent on the environment (Zhu *et al.*, 2013; Gleason *et al.*, 2016; Zhang *et al.*, 2019; Liu *et al.*, 2021). Other xylem traits such as vessel density (VD), lumen fraction, theoretical conductivity, vulnerability index (VI), wood density (WD), vessel grouping index (VGI), and the cell wall thickness to vessel diameter ratio $(t/b)^2$ have been linked to embolism resistance and inform hydraulic strategies (Hacke *et al.*, 2001; Levionnois *et al.*, 2021; Apgaua *et al.*, 2022). In addition, plants adapt to environments through an optimal combination of traits, indicated by different trait correlations or trade-offs (Wright *et al.*, 2007; Chave *et al.*, 2009). As an example, WD was negatively related to vessel diameter (Fajardo *et al.*, 2022; Carvalho *et al.*, 2023), theoretical hydraulic conductivity (Fajardo *et al.*, 2022; Y. B. Zhang *et al.*, 2022), and VI (Alvarado & Terrazas, 2023; Carvalho *et al.*, 2023). Furthermore, WD was positively associated with $(t/b)^2$ (Hacke *et al.*, 2001) and VD (Y. B. Zhang *et al.*, 2022; Carvalho *et al.*, 2023). In addition, the VGI was negatively correlated with mean vessel diameter (MVD), and positively related to VD (Levionnois *et al.*, 2021; Y. Zhang *et al.*, 2022). These xylem traits and their relationships are crucial in investigating hydraulic strategies and ecological adaptation across species and environments. Yet, comparative studies on the hydraulic traits of mistletoes and their hosts remain scarce, and the generality of these trait associations in parasitic plants is still unconfirmed.

Plants adjust their hydraulic architecture in response to environmental changes, with xylem trait variations being vital to their ecological adaptation strategies (Johnson *et al.*, 2018; Liang *et al.*, 2019; Garcia *et al.*, 2021; Shen *et al.*, 2023). Recent research indicates that vessel diameter and density vary across climatic gradients; species from wetter and warmer regions display larger vessels for efficient transport (Hacke *et al.*, 2017; Fontes *et al.*, 2022), while those from drier or colder habitats develop smaller, denser vessels for embolism resistance (Zanne *et al.*, 2014; Pfautsch *et al.*, 2016; Hacke *et al.*, 2017; Olson *et al.*, 2020). It has been found that WD increases in drier and colder environments (Chave *et al.*, 2009; Liang *et al.*, 2019), and species adapted to these conditions often show distinct hydraulic adaptations, such as networks of small conduits or leaf shedding (Carlquist, 1984; Zanne *et al.*, 2014). However, the variation in hydraulic architecture of predominantly evergreen mistletoes across environments is not well understood. Investigating the xylem traits of mistletoes and their hosts is crucial for understanding their water use strategies and how they respond to climate change in various environments.

Despite the growing importance of functional traits in ecological research, their measurements and understanding in parasitic plants, especially mistletoes, are still limited compared with other plant groups (Haynes, 2022; Teixeira-Costa *et al.*, 2023). Research on mistletoes has predominantly focused on their detrimental effects on hosts (Zweifel *et al.*, 2012; Ozturk *et al.*, 2019; Griebel *et al.*, 2022), with limited studies on their functional traits (Fajardo, 2022; Sibinelli & Ceccantini, 2022; Teixeira-Costa *et al.*, 2023; Zhang *et al.*, 2023). Fajardo (2022) observed that mistletoes have higher WD than trees and lianas, possibly due to higher xylem tensions in mistletoes, but highlighted the paucity of comparative studies on WD and xylem tension-related traits between mistletoes and their hosts. To date, only Gebauer *et al.* (2019) compared the xylem structure and function of petioles and twigs between mistletoe *Loranthus europaeus* Jacq. and its host *Quercus pubescence* Willd., revealing that mistletoe had a lower conduit lumen area, xylem area, xylem-to-cross-section area ratio and theoretical hydraulic conductivity than its host. However, comprehensive studies comparing the hydraulic adaptation strategies of mistletoes and their hosts in different environmental conditions, considering a broader range of xylem anatomical traits, are still lacking.

Increasing frequency and severity of droughts in southwestern China mirror the critical impact of water limitations on plant survival, growth, and mortality (Chen *et al.*, 2021; Yang *et al.*, 2023). This study focuses on xylem traits related to plant hydraulic function to discern the adaptive strategies of mistletoes and their hosts along a gradient of aridity index (proxy of diverse water and temperature conditions). We present the first comprehensive regional dataset, encompassing 12 xylem traits related to hydraulic efficiency, mechanical strength, and safety, in 119 mistletoe–host species pairs (340 individual pairs) across four ecologically distinct sites in Yunnan Province, China. Our research aims to unravel the ecological strategies of mistletoes and their hosts in contrasting environments, addressing the following questions and associated hypotheses:

(**1**) Do mistletoes and their host plants show differences in xylem traits and hydraulic safety-efficiency strategies? We hypothesize that mistletoes, due to their lower leaf water potentials and high xylem tension, prioritize hydraulic safety over efficiency. This implies that mistletoes would exhibit traits associated with lower hydraulic efficiency (such as smaller vessel diameter and theoretical hydraulic conductivity) and enhanced hydraulic safety (such as greater VD and WD).

(**2**) Are trait coordination and trade-offs in xylem traits consistent between mistletoes and their hosts? Due to limitations in xylem space and resources, different xylem traits are expected to show coordination or trade-offs. Therefore, we expect a hydraulic efficiency-safety trade-off in both mistletoes and their hosts. However, given the unique water acquisition strategies of mistletoes, some coordination or trade-offs in mistletoes would be weaker than those of their hosts.

(**3**) Do the hydraulic traits of both mistletoes and hosts vary in unison across aridity gradients? Do hosts influence the hydraulic traits of mistletoes across sites? We hypothesize that environmental variations in water availability and temperature act as common selection drivers for both mistletoes and hosts, influencing xylem development and affecting the comparative analysis of xylem traits between them, thus leading to a differentiation in xylem traits across sites. In addition, we expect that host hydraulic efficiency (water supply to mistletoes) influences mistletoe xylem traits. Both mistletoes and hosts are expected to exhibit

Table 1 List of xylem traits measured, abbreviations, units, and their ecophysiological significance.

Trait	Abbreviation	Unit	Ecological significance
Maximum vessel diameter	Dmax	µm	Water transport efficiency and storage (Poorter *et al*., 2010; Méndez-Alonzo *et al*., 2012; Chen *et al*., 2020)
Mean vessel diameter	MVD	µm	
Hydraulically weighted vessel diameter	D_h	µm	
Theoretical hydraulic conductivity	K_t	$\mathrm{kg\,m^{-1}\,s^{-1}\,MPa^{-1}}$	
Vessel area fraction	VAF	%	
Saturated xylem water content	SXWC	%	
Vulnerability index	VI	–	Water transport safety and mechanical strength (Hacke *et al*., 2001; Carlquist, 2009; Shen *et al*., 2023)
Vessel density	VD	$\mathrm{no.\ mm^{-2}}$	
Conduit double wall thickness	CWT	µm	
Conduit wall reinforcement	CWR	–	
Vessel grouping index	VGI	–	
Wood density	WD	$\mathrm{g\,cm^{-3}}$	

larger vessel diameters and lower WD in warm and wet habitats, while in dry-hot and/or cold habitats, constraints of water deficits and subzero-temperature stresses would result in smaller vessel diameters, higher VD, and higher sapwood density.

Materials and Methods

Sites and species

Our research was carried out in four distinct locations in Yunnan Province, China, namely Lijiang, Ailaoshan, Xishuangbanna, and Yuanjiang, each with unique climatic conditions. Notably, the mean annual precipitation exhibited a significant range, stretching from 733 mm to as much as 1778 mm among these sites. Similarly, the mean annual temperatures at these locations showed marked differences, with Lijiang recording 7.2°C, Ailaoshan 11.3°C, Xishuangbanna 22.7°C, and Yuanjiang 24.7°C. The aridity index is the ratio of annual precipitation to annual potential evapotranspiration. Consequently, the smaller the value is, the more arid the environment is. The aridity indices for Lijiang, Ailaoshan, Xishuangbanna, and Yuanjiang were 1.62, 1.44, 0.96, and 0.33, respectively. A higher proportion of the precipitation falls during the monsoon season, which typically spans from May to October. Detailed climate and soil characteristics of these sites are shown in Zhang *et al.* (2023).

The species selection criteria focused on the most common and representative mistletoes at each site, including both generalist and specialist species. Host plants varied in growth form, encompassing trees, shrubs, and lianas, and in leaf habits, including evergreen and deciduous types, while mistletoes were mainly evergreen hemiparasitic plants. The heights of the hosts ranged from 3 to 20 m, and their diameters at the breast height ranged from 10 to 50 cm. In Lijiang, Ailaoshan, and Yuanjiang, our collection focused on mistletoe–host species pairs from secondary forests with relatively open canopies, along roadsides and in habitats subjected to disturbance, where mistletoe infection rates exceeded those in pristine forests. Conversely in Xishuangbanna, mistletoe–host pairs were collected from a common garden with most hosts in open environments (Xishuangbanna Tropical Botanical Garden, hereafter XTBG). Overall, we sampled a total of 119 mistletoe–host species pairs (340 replicates), including mistletoes from two families, seven genera, and nine species, and host plants from 40 families, 77 genera, and 101 species (Supporting Information Tables S1, S2).

Our methodology for selecting host individuals with mistletoe infection was referred to previous research (Scalon & Wright, 2015; Richards *et al.*, 2021; Zhang *et al.*, 2023). Mostly, host species were infected by one mistletoe species, but some had two different mistletoes (Table S2). Sampling typically involved three individuals per mistletoe–host species pair, but sometimes, only one or two infected hosts per pair were available. Samples included mistletoes and host samples from noninfected branches on the same plant. Fieldwork was conducted during the rainy season of 2019, from August to October.

Xylem traits

We measured 12 xylem traits associated with water transport efficiency, hydraulic safety, and mechanical strength (Table 1). All mistletoes sampled were in a state of sexual maturity, indicated by the presence of flowers and fruits. According to Sibinelli & Ceccantini (2022), Loranthaceae mistletoes mature early, with minimal differences between juvenile wood, characterized by greater cell variation, and mature wood, characterized by more consistent cell sizes and organization. They suggest that these mistletoes develop mature wood in slender branches for efficient nutrient transfer after seedling establishment. This uniformity in wood anatomy across slender branches allows for valid anatomical comparisons across samples (Sibinelli & Ceccantini, 2022). For each mistletoe–host individual pair, we harvested two branches exposed to direct sunlight from the outermost part of the canopy for the mistletoes and hosts using a pole pruner. For the hosts, we selected the branches without any mistletoe infection but at a similar canopy position as the mistletoe branches we sampled. Most mistletoe samples were taken from the middle to upper portions of the host crown, as this is where mistletoes typically parasitize. In case of hard-to-reach branches, climbing and extended pole pruners (exceeding 5 m in length) were used. Upon collection, the branches were enclosed in dampened paper towels, securely placed in plastic bags, and transported to the laboratory.

For twig sampling, two segments *c.* 30–50 cm below the apex, each *c.* 0.8–1 cm in diameter, were chosen to minimize the effect of stem diameter on vessel dimensions (Olson *et al.*, 2014). For mistletoe branches, the length varies among different species, and among individuals of the same species. We tried to sample the middle to lower portion of the longest branch within an individual. These segments were stripped of bark and pith, submerged in distilled water for 24 h to be saturated, and then their volume was measured using the water displacement method. After saturation, they were weighed, oven-dried at 80°C for 72 h to a constant mass, and weighed again. Wood density ($\mathrm{g\,cm^{-3}}$) was calculated as the dry mass to saturated volume ratio, and saturated xylem water content (SXWC, %) as the ratio of saturated minus dry mass to saturated mass (Méndez-Alonzo *et al.*, 2012). Additional wood samples were preserved in a solution of 50 ml formalin, 50 ml 17.5 $\mathrm{mol\,l^{-1}}$ glacial acetic acid, and 900 ml 70% alcohol for subsequent anatomical measurements.

Twig segments, each measuring 2–3 cm in length, were smoothly flattened using a razor blade and subsequently imaged directly using an automatic digital microscope (ZEISS Smart zoom 5, Jena, Germany), instead of using traditional sectioning techniques. Each sample was photographed, focusing on a wedge-shaped area within the field of view of the microscope. We used a set of 12 images from three distinct individuals to assess vessel diameter and density for each species pair. For species with fewer than three individuals, additional images per individual were taken in an effort to obtain more accurate measurements. Vessel lumens within the wedge were precisely outlined to sharpen the image for better differentiation of vessels from other tissues using the PhotoShop CS5 (Adobe Systems, San Jose, CA, USA). Thereafter, using ImageJ software (US National Institutes of Health, Bethesda, MD, USA), we quantified the number and area of the vessels in each unit area of the image. Vessels at the edges, if less than half of a vessel or very small, were excluded from the count. Vessel diameter was determined following the method of Meunier *et al.* (2020):

$$D_i = 2\sqrt{\left(\frac{A_i}{\pi}\right)} \qquad \text{Eqn 1}$$

where A_i ($\mu\mathrm{m}^2$) represents the surface area of a vessel, π is 3.14. Mean vessel diameter (μm) was calculated by summing the diameters of all vessels and then dividing by their total number. The maximum vessel diameter (D_{max}, μm) is calculated by averaging the diameters of the 10 largest vessels observed. Hydraulically weighted vessel diameter (D_{h}; μm) was calculated following the method described by Poorter *et al.* (2010):

$$D_{\mathrm{h}} = \left[\left(\frac{1}{n}\right)\sum_{i=1}^{n} D_i^4\right]^{\frac{1}{4}} \qquad \text{Eqn 2}$$

Vessel density (no. $\mathrm{mm^{-2}}$) and vessel area fraction (VAF; %) were calculated by counting the number of vessels per unit area and the proportion of area occupied by vessels, respectively.

Theoretical hydraulic conductivity (K_{t}, $\mathrm{kg\,m^{-1}\,s^{-1}\,MPa^{-1}}$) was computed according to Poorter *et al.* (2010):

$$K_{\mathrm{t}} = \left(\frac{\pi\rho}{128\eta}\right) \times \mathrm{VD} \times D_h{}^4 \qquad \text{Eqn 3}$$

where ρ is the water density (998.2 $\mathrm{kg\,m^{-3}}$), and η is the water viscosity (1.002×10^{-9} MPa s) at 20°C. The K_{t} is usually higher than measured hydraulic conductivity due to ignoring the resistance of vessel perforation plates, pit aperture, and embolized vessels. However, correlations between anatomically based conductivity and actual hydraulic measurements are generally consistent across species, as demonstrated in previous studies (Chen *et al.*, 2020; Kawai *et al.*, 2021).

Conduit wall reinforcement (CWR) was calculated using Hacke *et al.* (2001) formula, $\mathrm{CWR} = (t/b)^2$, with 't' as the vessel wall thickness between two adjacent vessels and 'b' as the vessel lumen diameter. For accuracy, vessels with clearly identifiable walls were used for measuring wall thickness, with over 20 vessels measured per species. Vessel wall thickness (CWT; μm) is an important functional trait that represents mechanical strength (Hacke *et al.*, 2001; Castelar *et al.*, 2023).

The VGI is calculated by dividing the aggregate number of vessels by the number of vessel groups (i.e. with vessel groups including both solitary vessels and groups of vessels with true wall-by-wall contact; Carlquist, 2009; Scholz *et al.*, 2013). Consequently, a higher index value indicates a greater degree of vessel connectivity, whereas values close to 1 suggest a predominance of isolated vessels (Scholz *et al.*, 2013).

Carlquist's VI is defined as the ratio of MVD and VD, commonly used to assess the vulnerability of the xylem to embolism (Carlquist, 1977; Scholz *et al.*, 2013). Lower VI value indicates safer water transport (Carlquist, 1977; Shen *et al.*, 2023). This index also estimates the degree of xeromorphy of the xylem and is the anatomical counterpart of water potential at 50% conductivity loss (Ewers *et al.*, 2023).

Data and statistical analyses

All analyses were conducted in R 4.2.2 (R Core Team, 2023). Traits with multiple values per individual were averaged, and then re-averaged across individuals per species. All data were $\log_{10}$-transformed to improve the normality and homogeneity of variances. We used linear mixed models (LMMs) to test the effects of life form (mistletoe *vs* host) and site (Lijiang, Ailaoshan, XTBG, and Yuanjiang) on xylem traits. To test whether the mistletoes in this study exhibit lower water use efficiencies and a more water-spending strategy than their hosts, contributing to a better understanding of the hydraulic adaptation paradox in mistletoes, the stable carbon isotope (δ^{13}C) data were derived from Zhang *et al.* (2023) and reanalyzed here. We included life form, site, and their interactions as fixed effects. Species pairs and species were introduced in models as random effects to account for pseudo-replication. When significant differences were detected, *post hoc* multiple comparisons were performed to

Table 2 Effects of life form and site on the xylem traits analyzed using linear mixed-effects model.

	Fixed effects						Random effects				
	Life form		Site		Life form × Site		Species pairs		Species		
Traits	*F*	*P*	*F*	*P*	*F*	*P*	LRT	Pr (>Chisq)	LRT	Pr (>Chisq)	Marginal r^2/ Conditional r^2
$D_{\max}$	10.33	**0.002**	6.77	< **0.001**	3.44	**0.018**	14.40	< **0.001**	967.16	< **0.001**	0.461/0.975
MVD	8.65	**0.004**	7.45	< **0.001**	2.97	**0.034**	43.75	< **0.001**	734.25	< **0.001**	0.491/0.963
D_h	9.04	**0.003**	6.70	< **0.001**	2.85	**0.040**	30.96	< **0.001**	851.15	< **0.001**	0.478/0.970
K_t	23.91	< **0.001**	7.69	< **0.001**	4.81	**0.003**	42.25	< **0.001**	541.24	< **0.001**	0.525/0.942
VAF	21.07	< **0.001**	13.25	< **0.001**	3.04	**0.031**	50.37	< **0.001**	312.20	< **0.001**	0.469/0.886
SXWC	10.24	**0.002**	6.18	**0.001**	3.03	**0.032**	44.27	< **0.001**	195.11	< **0.001**	0.229/0.785
VI	4.50	**0.036**	42.83	< **0.001**	NS		45.44	< **0.001**	946.46	< **0.001**	0.543/0.974
VD	0.33	0.569	6.67	< **0.001**	2.61	**0.054**	58.58	< **0.001**	762.14	< **0.001**	0.422/0.965
CWT	1.12	0.293	8.24	< **0.001**	3.42	**0.019**	183.36	< **0.001**	289.74	< **0.001**	0.312/0.908
CWR	8.41	**0.005**	8.15	< **0.001**	4.20	**0.008**	194.01	< **0.001**	86.05	< **0.001**	0.167/0.741
VGI	75.27	< **0.001**	6.20	**0.001**	NS		118.95	< **0.001**	186.26	< **0.001**	0.547/0.878
WD	9.69	**0.002**	11.18	< **0.001**	NS		70.43	< **0.001**	524.83	< **0.001**	0.243/0.905

The fixed factors were life form (mistletoe vs host), site (Lijiang, Ailaoshan, XTBG, and Yuanjiang) and their interactions and their values were *F* and *P*-values. The random factors were species pairs and species and their values were likelihood ratio and Pr (>Chisq)-values. 'NS' indicates nonsignificant interaction term, which was dropped off during model selection. Marginal r^2 and conditional r^2 were the variation explained by fixed effects and the variation explained by both fixed and random effects, respectively. Bold font indicates significant term. See Table 1 for trait abbreviations.

identify trait variation between life forms and among sites. The postmultiple comparisons were done using the 'EMMEANS' package (Lenth, 2021). The degrees of freedom were calculated using the Kenward-Roger method, and the Bonferroni method was used to adjust the *P* value during multiple comparisons. Further, we also conducted the LMMs by replacing 'site' with the 'aridity index' to test the effect of aridity. We fitted LMMs using the *lmer* function of the 'LME4' package (Bates *et al*., 2015). The normality and homogeneity of residuals were checked using the *check_model* function from the 'PERFORMANCE' package (Lüdecke *et al*., 2021), and predicted values and 95% confidence intervals were extracted for plotting using the 'EMMEANS' package. We quantified the proportion of variance explained by the models with the marginal r^2 (for the fixed effects) and the conditional r^2 (for the fixed and random effects combined; Nakagawa & Schielzeth, 2013; Bartoń, 2020).

We utilized the Permutational Multivariate Analysis of Variance (PERMANOVA; Anderson, 2001) on mean data of species pairs to determine if mistletoes and host plants have distinct trait spaces at various sites, with the analysis involving 1000 permutations. The full model included life form, site, and their interactions. Analyses were conducted using the *adonis* function in the 'VEGAN' package (Oksanen *et al*., 2013). Subsequently, a principal component analysis (PCA) was performed to visualize the spatial distribution of multidimensional traits across different life forms and sites. For the PCA, mistletoe–host pairs with missing data were excluded, resulting in 115 pairs being analyzed. The PCA was executed using the *princomp* function in the STATS package. Lastly, we conducted similar analyses based on each site dataset to check whether mistletoes and hosts occupied different trait spaces.

We used Pearson correlation analysis to examine relationships between xylem traits, and standardized major axis (SMA) analysis (Warton *et al*., 2012) to assess whether these relationships significantly varied between mistletoes and their hosts in terms of slopes, intercepts, and shifts. To ascertain whether mistletoes displayed trait variations distinct from the host plants they parasitized, we also tested whether the slope of each xylem trait in mistletoes *vs* their hosts differed from one and intercepts differed from zero.

Results

Differences in xylem traits between mistletoes and hosts

Both fixed and random effects significantly explained the variance in all 12 xylem traits (Table 2), with models incorporating random effects (species pairs and species) demonstrating a better fit (lower AIC values; Table S3). Of the fixed effects, 10 traits differed significantly between life forms, and 12 xylem traits differed significantly among sites. There were significant interactions between life form and site on nine out of the 12 xylem traits, except for VI, VGI, and WD (all $P < 0.05$; Fig. 1; Tables 2, S4). The maximum vessel diameter ($D_{\max}$), MVD, hydraulically weighted vessel diameter (D_h), theoretical hydraulic conductivity (K_t), VAF, SXWC, and VI of mistletoes were significantly lower than those of the host plants. Vessel density and conduit wall thickness (CWT) did not show significant differences between life forms, but the interaction of life form and site had a significant effect on them. Moreover, mistletoes had significantly higher VGI, CWR, and WD than their hosts. Interestingly, $D_{\max}$, MVD, D_h, K_t, and VAF between mistletoes and hosts were more divergent in the wet-hot (XTBG) and dry-hot (Yuanjiang) sites, with no significant differences in the two wet colder sites (Lijiang and Ailaoshan), except for K_t and VAF, which differed significantly in Ailaoshan. Additionally, mistletoes had lower $\delta^{13}C$ values than their hosts across four sites (Fig. 2). The coefficient of variation for the majority of xylem traits was higher in hosts than

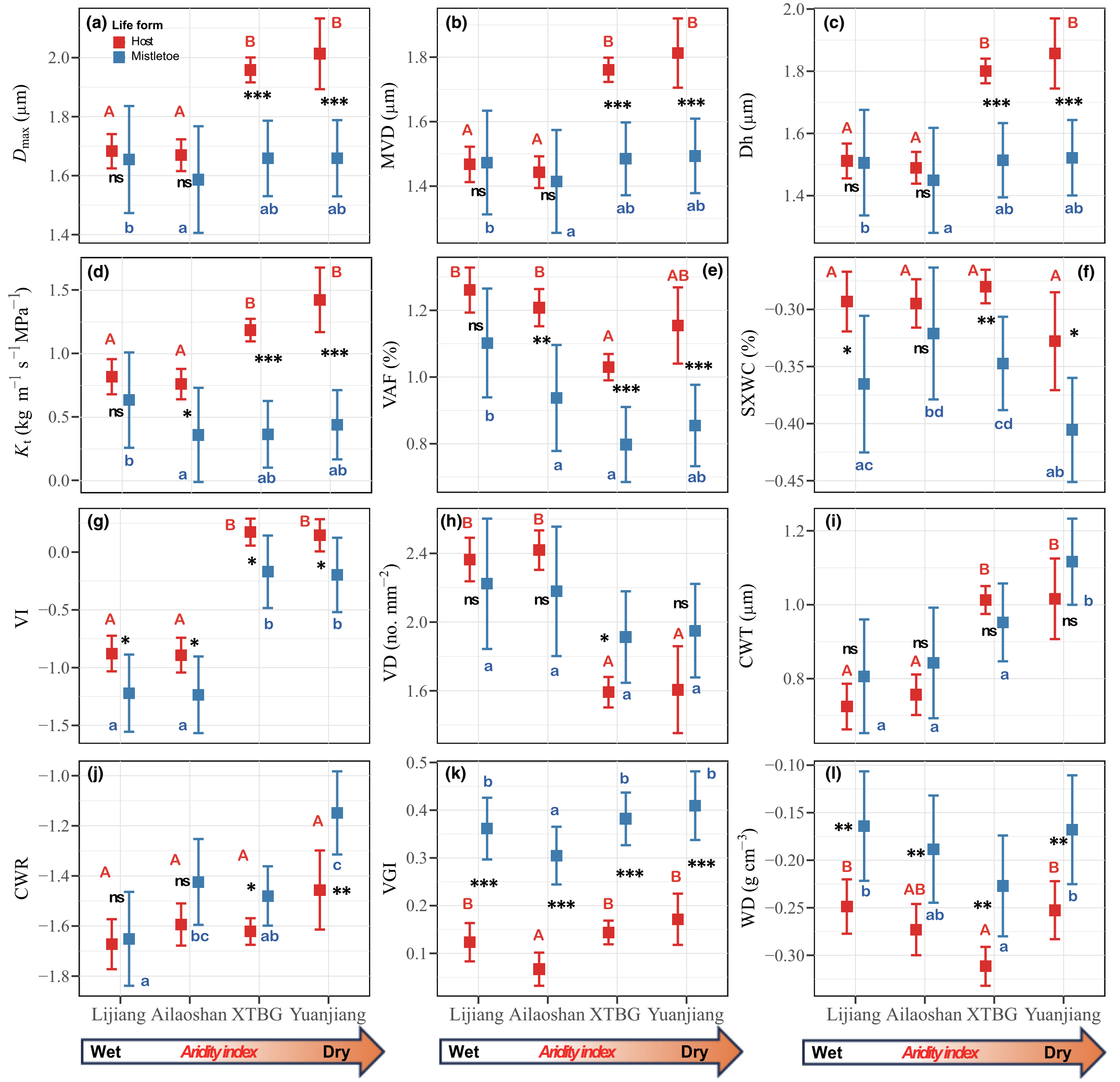

Fig. 1 Differences in xylem traits among mistletoes and hosts from four sites. (a) maximum vessel diameter (D_{max}), (b) mean vessel diameter (MVD), (c) hydraulically weighted vessel diameter (D_h), (d) sapwood theoretical conductivity (K_t), (e) vessel area fraction (VAF), (f) saturated xylem water content (SXWC), (g) vulnerability index (VI), (h) vessel density (VD), (i) conduit double wall thickness (CWT), (j) conduit wall reinforcement (CWR), (k) vessel grouping index (VGI), and (l) wood density (WD). Means and 95% confidence intervals (as shown by horizontal bars) are shown based on predictions from linear mixed-effects models. Red and blue colors indicate hosts and mistletoes, respectively. The black '*' indicates a significant difference between mistletoes and hosts for a given xylem trait within the same site, while 'ns' indicates nonsignificance. Different red uppercase letters indicate significant differences in a given xylem trait among hosts across the four sites, while different blue lowercase letters indicate significant differences in a given xylem trait among mistletoes across the four sites. All variables were $\log_{10}$-transformed before analysis. *, $P < 0.05$; **, $P < 0.01$; ***, $P < 0.001$.

in mistletoes, except for CWR and VGI (Fig. S1). When 'site' was replaced with 'aridity index' in the LMMs, some changes were observed. The interactions between life form and aridity index for certain traits, such as VAF, SXWC, and CWT, were no longer significant (Table S5). Conversely, the previously non-significant interaction for some traits, such as VI and WD, became significant. The comparative differences between mistletoes and their hosts remained largely unchanged. However, VD,

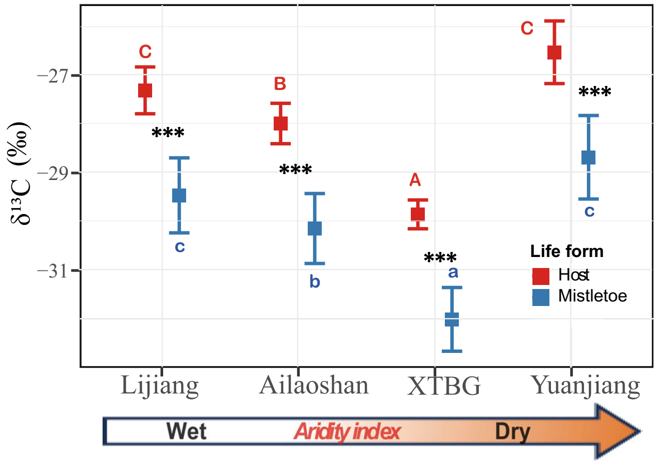

Fig. 2 Differences in the stable carbon isotope (δ^{13}C) among mistletoes and hosts across four sites. Data are obtained from Zhang *et al*. (2023) and were reanalyzed with life form and site as fixed effects (due to the nonsignificant interaction between them), and species and species pairs as random effects. Means and 95% confidence intervals (as shown by horizontal bars) are shown based on predictions from linear mixed-effects models. Red and blue colors indicate hosts and mistletoes, respectively. The black '*' indicates a significant difference between mistletoes and hosts for a given xylem trait within the same site; ***, $P < 0.001$. Different red uppercase letters indicate significant differences in a given xylem trait among hosts across the four sites, while different blue lowercase letters indicate significant differences in a given xylem trait among mistletoes across the four sites.

which was previously nonsignificant, showed a significant difference (Table S5).

Life form and site were distinctly separated in the sampled multidimensional functional space (both $P < 0.05$; Table 3). The variance explained by site, life form, and their interaction was 38.9%, 20.9%, and 4.8%, respectively. PCA results, based on 12 xylem traits from 115 mistletoe–host species pairs across four sites (Fig. 3), corroborated the results of LMMs based on individual data (Table 2) and of PERMANOVA based on mistletoe–host pair mean data (Table 3). The first two principal components accounted for 54.7% and 21.7% of the total variance, respectively (Fig. 3). Species distribution along the first axis was positively associated with higher K_t, D_{max}, MVD, D_h, VI, and CWT, and negatively correlated with VD (Fig. 3; Table S6). Along the second axis, species distribution was positively related to VAF and SXWC, and negatively related to CWR, VGI, and WD. Mistletoes and hosts tended to occupy different regions of the multi-trait space. Specifically, mistletoes were located at the negative positions of the first and second axes, representing a conservative hydraulic strategy (relatively high hydraulic safety and low efficiency), whereas hosts were in the opposite location. When we considered life form in each site, the pattern was consistent with PCA results across the four sites (Fig. S2). Mistletoes and hosts were also distinctly divergent in the multi-trait space at each site, with mistletoes having traits related to lower hydraulic efficiency and higher resistance to xylem embolism, and hosts showing the opposite pattern (Fig. S2; Table S7).

Table 3 PERMANOVA on the Euclidean distance of 12 xylem traits for 115 mistletoe–host species pair mean values.

Source	Degree of freedom	Sum of squares	*F*	r^2	*P*
Life form	1	45.95	131.67	0.209	< **0.001**
Site	3	85.39	81.57	0.389	< **0.001**
Life form × Site	3	10.57	10.10	0.048	< **0.001**
Residual	222	77.47		0.353	
Total	229	219.38		1	

Life forms, sites, and their interactions were explanatory variables. The response variables were 12 traits. Bold font indicates significant term.

Associations among xylem traits of mistletoes and hosts

Host WD, a functional trait highly associated with xylem structure and function, was significantly and negatively correlated with D_{max}, MVD, D_h, K_t, and VI, and positively associated with VD, VGI, and CWR (Figs 4, S3). Interestingly, these correlations were not significant in mistletoes. Both mistletoes and host plants showed a significantly negative correlation between SXWC and WD, with mistletoes displaying a less steep slope in this relationship (Fig. 4; Table S8).

A significant positive correlation was found between D_h and K_t in both mistletoes and hosts, although hosts exhibited a notably higher intercept (Fig. 5; Table S8). D_h was negatively correlated with VD and VAF in both mistletoes and hosts, with the latter exhibiting a steeper slope in both instances. Furthermore, a strong positive correlation was identified between D_h and VI, with mistletoes having a steeper slope. D_h was also positively correlated with CWT and VGI in both groups, with a steeper slope observed in mistletoes. VD and K_t were negatively correlated in both life forms, with hosts showing a higher intercept and shift toward the left. VD was also positively related to VAF, with mistletoes demonstrating a steeper slope. Lastly, VD and VI exhibited a significant negative correlation in both, with a steeper slope in mistletoes.

A significant negative correlation was observed between VD and VGI in both mistletoes and hosts, with mistletoes exhibiting a steeper slope (Fig. 6; Table S8). There was a positive correlation between VI and K_t in both groups, with hosts displaying a higher intercept and shift toward the right. CWR was negatively linked with K_t in mistletoes, with marginal significance in hosts. Both mistletoes and hosts displayed a positive correlation between VGI and K_t, with hosts having a steeper slope. While K_t and SXWC were negatively correlated in mistletoes, a positive correlation was noted in hosts. VI showed a negative relationship with VAF and a positive one with VGI in both, with hosts having a steeper slope. Lastly, VGI and CWR were negatively correlated in both, with marginal significance in hosts.

Variation in xylem traits in mistletoes and hosts across sites

Site significantly influenced all xylem traits in both hosts and mistletoes (Fig. 7; Table 2), and the aridity index also showed significant influences, except for VI and WD. However, we cannot

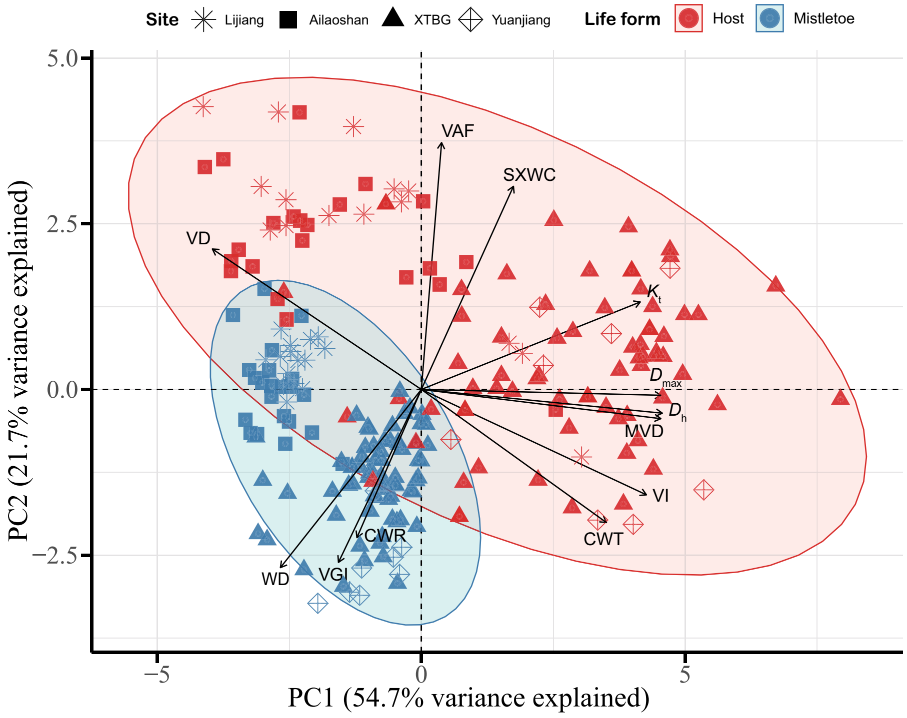

Fig. 3 Biplot of the first two axes of the principal component (PC) analysis for the 12 xylem traits and the loadings of the 115 mistletoe–host species pairs from Lijiang (star, $n = 15$), Ailaoshan (square, $n = 22$), Xishuangbanna Tropical Botanical Garden (triangle, $n = 70$), and Yuanjiang (diamond, $n = 8$). Red and blue colors indicate hosts and mistletoes, respectively. All variables were $\log_{10}$-transformed before analysis. See Table 1 for trait abbreviations.

preclude the influence of the aridity index on these traits due to the significant interaction between life form and aridity index (Fig. 8; Table S5). Both mistletoes and hosts exhibited either similar or divergent responses to different environments (Fig. 8). Specifically, host plants in Lijiang and Ailaoshan (two colder sites with a higher aridity index), as well as in XTBG and Yuanjiang (two warmer sites with a lower aridity index) showed no significant differences in D_{max}, MVD, D_{h}, and K_{t} (Figs 2, 8; Tables 2, S4), yet hosts in Lijiang and Ailaoshan had notably smaller values for these traits than those in XTBG and Yuanjiang. For mistletoes, significant differences in D_{max}, MVD, and D_{h} were only observed between Ailaoshan and Lijiang. Host VAF was lower in XTBG than in Lijiang and Ailaoshan, while mistletoe VAF was higher in Lijiang than in Ailaoshan and XTBG. SXWC and CWR in hosts showed no significant differences among sites, unlike in mistletoes. Host VD and CWT were consistent between Lijiang and Ailaoshan, and XTBG and Yuanjiang, with Lijiang and Ailaoshan exhibiting higher VD but lower CWT than XTBG and Yuanjiang. Mistletoe VD remained stable across sites, with Yuanjiang showing higher CWT. Mistletoes and hosts showed consistent variation patterns in VI, VGI, and WD across sites, with lower VI in Lijiang and Ailaoshan than in XTBG and Yuanjiang, lower VGI in Ailaoshan, and significant WD differences noted between Lijiang and XTBG, as well as XTBG and Yuanjiang.

The PERMANOVA results and PCA analyses revealed clear separations among the four sites for both mistletoe and host species (Fig. 7; Table S9). In the PCA, the first two axes accounted for 65.8% of the variance in mistletoes and 75.7% in hosts. For both mistletoes and hosts, similar trait spaces were observed in two wet colder sites (Lijiang and Ailaoshan), as well as in wet-hot (XTBG) and dry-hot (Yuanjiang) sites, but there was stronger divergence between these site pairs. Mistletoes and hosts in Lijiang and Ailaoshan had higher VD and VAF, while those in XTBG and Yuanjiang showed higher D_{max}, MVD, D_{h}, K_{t}, and VI (Tables S10, S11). Additionally, a positive correlation was found between each xylem trait in mistletoes and their hosts, except for SXWC, with slopes significantly different from 1 (Fig. S4).

Discussion

Our study, conducted across four sites with distinct environmental conditions, reveals a general divergence in hydraulic strategies between mistletoes and their hosts. Specifically, mistletoes with lower water use efficiency (lower δ^{13}C values) compared with their hosts are apparently more aggresive in water use, which is in line with previous findings (Scalon & Wright, 2015; Richards *et al.*, 2021; Zhang *et al.*, 2023). Moreover, mistletoes show higher hydraulic safety but lower efficiency than their hosts. The relatively low hydraulic efficiency in mistletoes seems to contradict their high transpiration (Yang *et al.*, 2017; Griebel *et al.*, 2022) and low water use efficiency. Thus, their high transpiration could be driven by a high driving force (low leaf water potentials) rather than a high hydraulic conductivity. The xylem traits of mistletoes are strongly influenced by the water supply efficiency of the hosts. The overall xylem trait relationships in mistletoes are different from those in hosts, suggesting different constraints on trait development and different ecological strategies.

Mistletoes have a more conservative hydraulic strategy than their hosts

Consistent with our first hypothesis, mistletoes had lower hydraulic efficiency and higher hydraulic safety than their hosts.

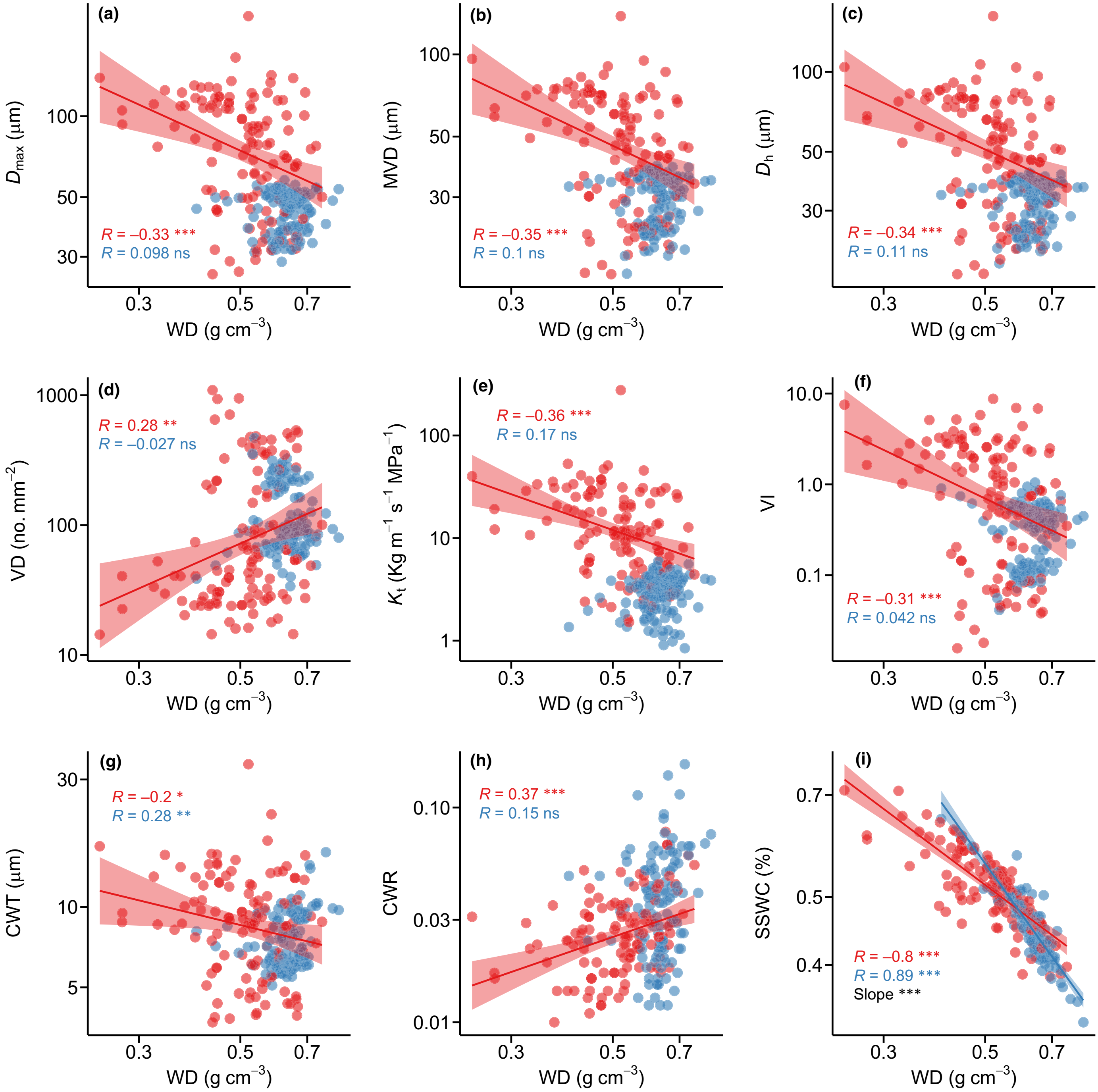

Fig. 4 Bivariate relationships between wood density (WD) with (a) maximum vessel diameter (D_{max}), (b) mean vessel diameter (MVD), (c) hydraulically weighted vessel diameter (D_h), (d) vessel density (VD), (e) theoretical hydraulic conductivity (K_t), (f) vulnerability index (VI), (g) conduit double wall thickness (CWT), (h) conduit wall reinforcement (CWR), and (i) saturated xylem water content (SXWC). Red and blue colors indicate hosts and mistletoes, respectively. Regression lines and confidence intervals are provided where bivariate correlations are significant. If significant correlations exist in both mistletoes and hosts, the slope, intercept, and shift between the two groups were tested using standardized major axis analysis. If the slope was significant, only the slope was reported; otherwise, the intercept and shift were provided. ns, $P > 0.05$; *, $P < 0.05$; **, $P < 0.01$; ***, $P < 0.001$.

The smaller maximum vessel diameter (D_{max}), MVD, hydraulically weighted vessel diameter (D_h), theoretical hydraulic conductivity (K_t), VAF, and SXWC all suggest lower hydraulic efficiency in mistletoes. By contrast, lower VI in mistletoes across four sites suggests their relatively higher embolism resistance (Ewers *et al*., 2023; Shen *et al*., 2023). Higher VGI, indicating a higher redundancy of the hydraulic pathway (Apgaua *et al*., 2022), in mistletoes compared with hosts across four sites, also suggests higher hydraulic safety (Carlquist, 1984; Lens *et al*., 2011). VGI was found to be correlated with embolism

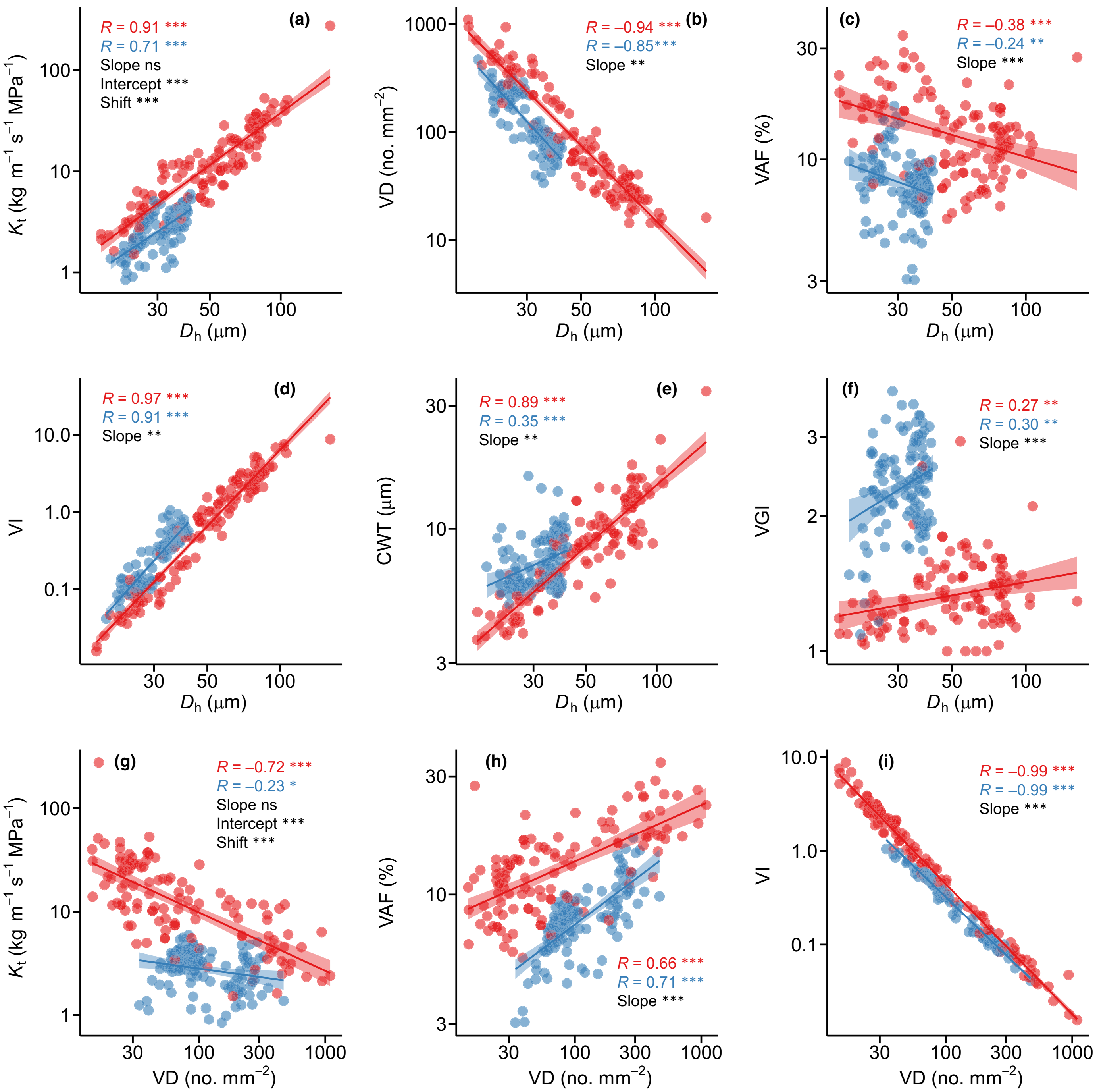

Fig. 5 Bivariate relationships between hydraulically weighted vessel diameter (D_h) with (a) theoretical hydraulic conductivity (K_t), (b) vessel density (VD), (c) vessel area fraction (VAF), (d) vulnerability index (VI), (e) conduit double wall thickness (CWT), and (f) vessel grouping index (VGI), and VD with (g) K_t, (h) VAF, and (i) VI. Red and blue colors indicate hosts and mistletoes, respectively. Regression lines and confidence intervals are provided where bivariate correlations are significant. If significant correlations exist in both mistletoes and hosts, the slope, intercept, and shift between the two groups were tested using standardized major axis analysis. If the slope was significant, only the slope was reported; otherwise, the intercept and shift were provided. ns, $P > 0.05$; *, $P < 0.05$; **, $P < 0.01$; ***, $P < 0.001$.

resistance in nonparasitic plants (Levionnois *et al.*, 2021; Y. Zhang *et al.*, 2022). This pattern agrees with the hydraulic efficiency vs safety trade-off partly mediated by vessel size (Hacke *et al.*, 2022; Isasa *et al.*, 2023). This trade-off across mistletoes and hosts is supported by both the overall and site-specific PCA results. Furthermore, higher CWR and WD in mistletoes than in hosts suggest a higher resistance to vessel implosion and mechanical strength (Hacke *et al.*, 2001; Liang *et al.*, 2021; Liu

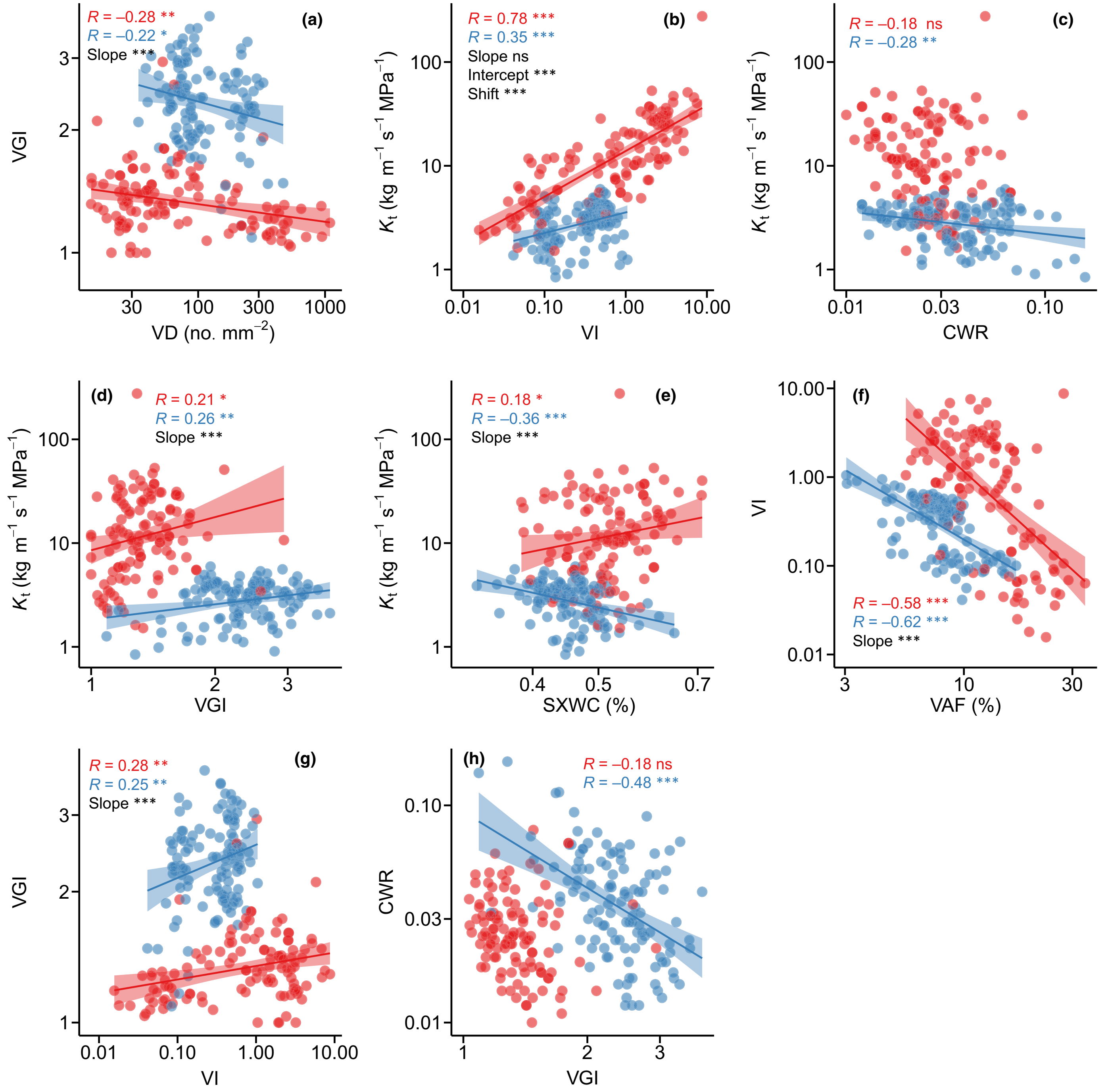

Fig. 6 Bivariate relationships between (a) vessel density (VD) and vessel grouping index (VGI), (b) vulnerability index (VI) and theoretical hydraulic conductivity (K_t), (c) conduit wall reinforcement (CWR) and K_t, (d) VGI and K_t, (e) saturated xylem water content (SXWC) and K_t, (f) vessel area fraction (VAF) and VI, (g) VI and VGI, (h) VGI and CWR. Red and blue colors indicate hosts and mistletoes, respectively. Regression lines and confidence intervals are provided where bivariate correlations are significant. If significant correlations exist in both mistletoes and hosts, the slope, intercept, and shift between the two groups were tested using standardized major axis analysis. If the slope was significant, only the slope significance was reported; otherwise, the intercept and shift were provided. ns, $P > 0.05$; *, $P < 0.05$; **, $P < 0.01$; ***, $P < 0.001$.

et al., 2024). Indeed, mistletoes experience high xylem tension compared with their hosts (Glatzel & Geils, 2009). In addition, mistletoes usually have a higher stomatal conductance and transpiration rate (Zweifel *et al.*, 2012; Yang *et al.*, 2017), resulting in lower leaf water potentials compared with terminal branches of their hosts (Glatzel & Geils, 2009; He *et al.*, 2021; Ye *et al.*, 2021). Therefore, mistletoes need to be more resistant to drought-induced embolism. Overall, these findings suggest that

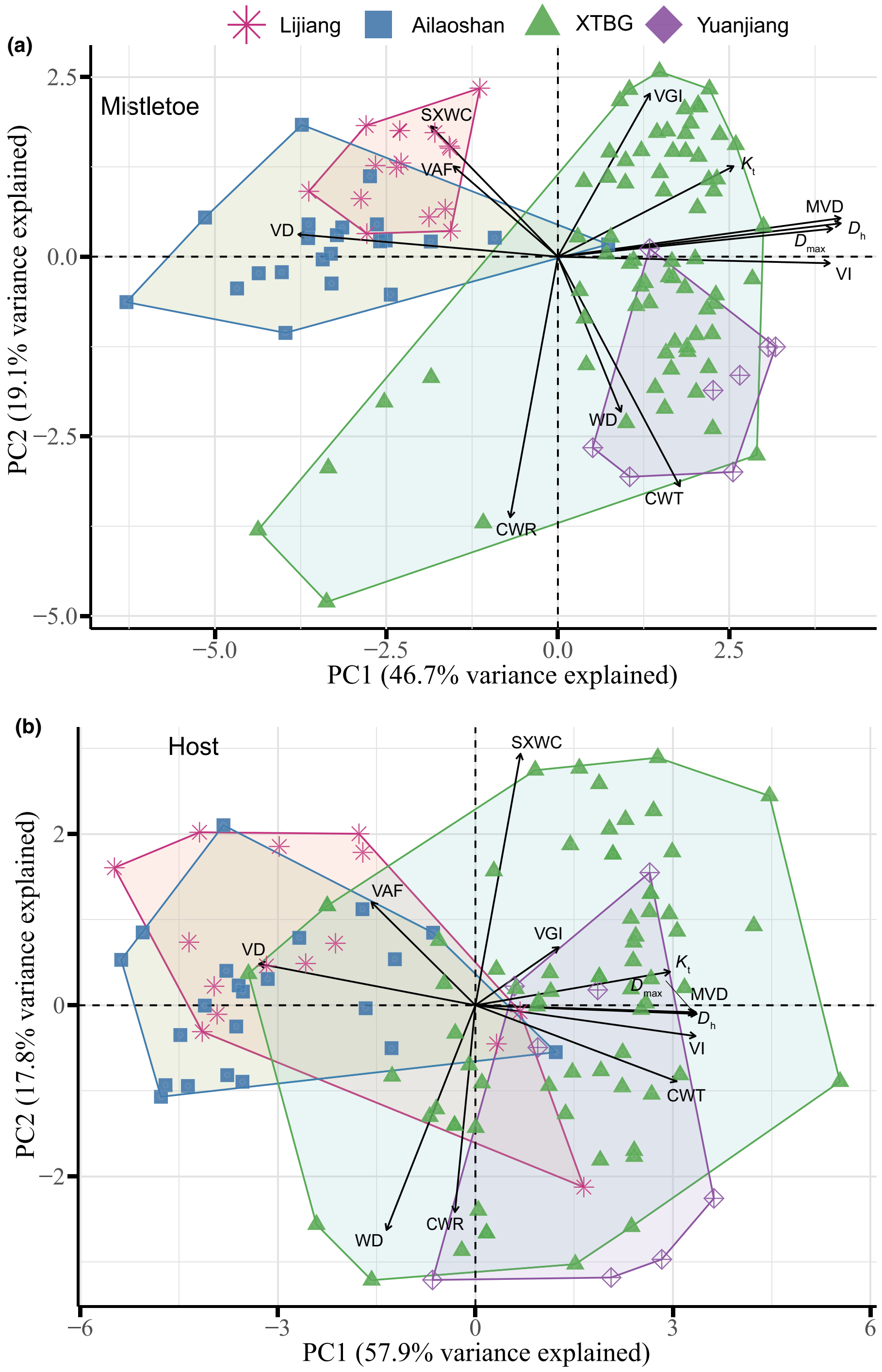

Fig. 7 Principal component analysis of 12 xylem traits for mistletoe and host species across four sites. Four sites were Lijiang (magenta star, $n = 15$), Ailaoshan (blue square, $n = 22$), Xishuangbanna Tropical Botanical Garden (green triangle, $n = 70$), and Yuanjiang (purple diamond, $n = 8$). The upper and lower panels are mistletoes and hosts, respectively. All variables were $\log_{10}$-transformed before analysis. See Table 1 for trait abbreviations.

mistletoes secure hydraulic safety in branches when facing the paradoxical challenge of the parasitic lifestyle (higher efficiency for higher stomatal conductance and transpiration *vs* higher safety needs due to high xylem tension). As xylem flow rate = water potential difference × hydraulic conductivity, the high xylem flow rate to support high transpiration in mistletoes could be maintained through low leaf water potentials rather than high hydraulic conductivity. Their stomatal control could be less responsive to declining water potentials compared with host plants, which could be tested in the future.

Mistletoes and hosts show different xylem trait relationships and ecological strategies

In mistletoes, the relationships between WD and xylem traits found in hosts were largely absent (except for SXWC), possibly due to smaller variations in xylem traits such as vessel size. The limited variations could be attributed to their relatively higher water stress (lower water potentials) that restricts the development of large vessels. It could also be partly explained by their terminal position in the soil–host–mistletoe hydraulic

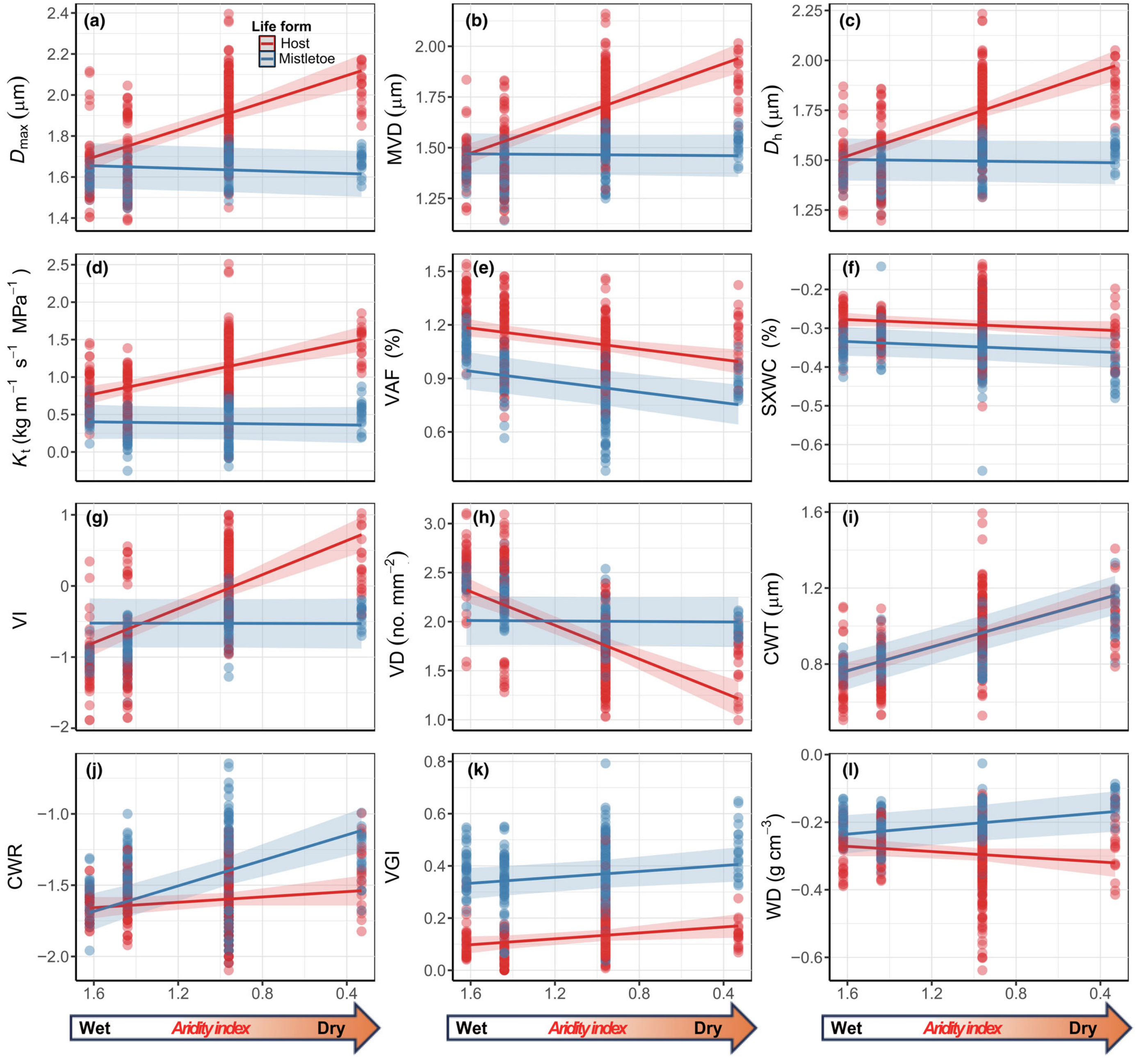

Fig. 8 Predicted xylem trait responses of mistletoes and their host plants across an aridity gradient using the results from linear mixed-effects models. The predictions were generated using the *ggpredict* function. The x-axis represents the aridity index, ranging from wet to dry conditions, and the y-axis shows the predicted values of 12 xylem traits. (a) maximum vessel diameter (D_{max}), (b) mean vessel diameter (MVD), (c) hydraulically weighted vessel diameter (D_h), (d) sapwood theoretical conductivity (K_t), (e) vessel area fraction (VAF), (f) saturated xylem water content (SXWC), (g) vulnerability index (VI), (h) vessel density (VD), (i) conduit double wall thickness (CWT), (j) conduit wall reinforcement (CWR), (k) vessel grouping index (VGI), and (l) wood density (WD). Red and blue colors indicate hosts and mistletoes, respectively, with shaded areas indicating the 95% confidence intervals. All variables were $\log_{10}$-transformed before analysis.

continuum, where the conduit diameters are known to decrease from the tree base to more distal parts of the branches (Anfodillo *et al*., 2006; Olson *et al*., 2020). For other pairwise trait correlations in both mistletoes and hosts, the different slopes or intercepts imply that mistletoes and hosts may differ in constraints on trait development and adopt different ecological strategies. For instance, D_h was negatively correlated with VD and VAF in both groups, with mistletoes showing steeper slopes, aligning with previous findings (Poorter *et al*., 2010; Y. B. Zhang *et al*., 2022). This negative correlation, indicative of a trade-off between hydraulic efficiency and safety (Islam *et al*., 2018), was more pronounced in mistletoes, as they exhibited a lower vessel diameter at a given VD. Additionally, VD negatively correlated with K_t in both mistletoes and hosts, with hosts showing higher K_t at given

VDs, indicating a lower hydraulic conductivity at a given VD in mistletoes.

The significant positive correlation between VI and K_t in both mistletoes and hosts, and the negative correlation between K_t and CWR in mistletoes all suggest the xylem efficiency and safety trade-off, as found in a previous study (Shen *et al*., 2023). CWR is linked to embolism resistance (Hacke *et al*., 2001), and a lower CWR suggests increased hydraulic risk (Guérin *et al*., 2020). Furthermore, mistletoes have higher vulnerability at a given diameter and lower vulnerability at a given VD compared with hosts. Overall, mistletoes exhibit a stronger trade-off between hydraulic efficiency and safety.

The unexpected positive relationships of VGI with D_h, K_t, and VI, negative relationships with VD and CWR in both mistletoes and their hosts contrast with previous findings that VGI was negatively correlated with vessel diameter, and positively related to VD (Levionnois *et al*., 2021; Y. Zhang *et al*., 2022). Although VGI is generally positively linked to embolism resistance (Levionnois *et al*., 2021; Y. Zhang *et al*., 2022; Carvalho *et al*., 2023), our findings indicate that higher VGI corresponds to increased hydraulic risk (higher VI and lower CWR). Earlier studies proposed that higher vessel interconnectivity, indicated by more grouped vessels, could lead to increased conductivity (Lens *et al*., 2011), which is supported by our observation of a positive correlation between VGI and K_t. Recent research suggests that vessel connectivity and grouping may enhance resistance to embolism spread without compromising hydraulic connectivity (Jupa *et al*., 2021; Mrad *et al*., 2021). Species with higher VGI may compensate for the hydraulic risk by reducing their vessel diameter and length, thereby reducing the possibility of embolism (Lens *et al*., 2011). Therefore, a higher VGI might enable mistletoes to maintain efficient water transport under favorable conditions and mitigate embolism risks in water-deficient scenarios, achieving a balance between hydraulic efficiency and safety. This adaptation could significantly enhance the presence and survival of mistletoes in diverse environments, particularly those with dry or cold seasons. Future research incorporating directly measured embolism resistance and mechanical strength could provide a more comprehensive understanding of the role of VGI in the regulation of water transport, especially in mistletoes.

Different responses of mistletoes and hosts to contrasting environments

Mistletoes and their hosts exhibited distinct responses to varying environments (Fig. 8), with hosts showing stronger responses in D_{max}, MVD, D_h, and K_t. The strong response in hosts aligns with research showing larger vessel diameters in warmer and wetter sites (Pfautsch *et al*., 2016; Hacke *et al*., 2017; Fontes *et al*., 2022), but contrasts with another study showing that plant height, not climate, was the driver of vessel diameter (Olson *et al*., 2018; Fajardo *et al*., 2020). As for mistletoes, their low water potentials and high resistance in the haustorium connection between mistletoes and their hosts (Goldstein *et al*., 1989) could constrain the development of large vessels, resulting in the limited variation of vessel diameter and K_t, and the responses to different environmental gradients in mistletoes. Higher VD but lower CWT of hosts at two colder sites compared with the warmer sites could probably provide greater hydraulic redundancy and a narrow diameter, both of which enhance resistance to freeze–thaw-induced embolism. By contrast, mistletoe VD remained consistent across all sites. This difference could be because mistletoe vessel traits, K_t, VD, and CWT may be more influenced by the hydraulic efficiency and water supply of their hosts, rather than by abiotic environmental factors alone. Moreover, unlike hydraulic efficiency-related traits, the VI of both mistletoes and hosts was lower in colder environments than in warmer sites. This could be attributed to the necessity for both hosts and mistletoes to adapt to freeze–thaw-induced embolism.

Interestingly, mistletoes and hosts exhibited similar hydraulic efficiency (D_{max}, MVD, D_h, K_t, and VAF) in two colder sites (Lijiang and Ailaoshan), while notable differences were observed in two warmer sites (XTBG and Yuanjiang). Such variation is primarily attributed to the significantly larger vessel sizes of hosts in warmer sites (XTBG and Yuanjiang), compared with those at the two colder sites. In colder climates, smaller host vessel diameters may be an adaptation to resist freezing-induced embolism (Hacke *et al*., 2017), resulting in no significant differences between mistletoes and hosts. By contrast, at the warmer sites (XTBG and Yuanjiang) without freeze–thaw events, hosts develop large vessel diameters to maximize hydraulic performance, while the development of large vessels in mistletoes is limited due to their lower water potentials and resistance in the haustorium, as discussed above.

Interactions between life form and site, and host effect on mistletoes

Consistent with our hypothesis, the interaction between life form (mistletoe vs host) and site significantly influenced nine out of the 12 xylem traits. This indicates that xylem trait comparisons between mistletoes and their hosts are intricately linked to specific sites and their environmental conditions. Moreover, the variance attributed to site differences surpassed that variance due to life form differences in the multidimensional trait space. These findings highlight the critical role of site and environmental conditions such as the aridity index in differentiating xylem traits between mistletoes and hosts, aligning with our earlier research on the effects of site environmental conditions on leaf nutrient and water relations (Zhang *et al*., 2023). Additionally, random effects, such as species pairs and species, accounted for a substantial portion of the variation in xylem trait comparisons, emphasizing species-specific responses and the unique nature of each mistletoe–host interaction. This is in line with previous studies on haustorium anatomy (Teixeira-Costa & Ceccantini, 2016) and leaf nutrient and water relations in mistletoes (Zhang *et al*., 2023). Therefore, both site effect and species-specific responses should be considered in future comparative studies between mistletoes and their hosts.

Hosts, as the biotic environment for mistletoes, may influence the variations and environmental responses of mistletoe xylem traits. Previous studies have shown that hosts affect mistletoe leaf functional traits (Zhang *et al*., 2023; Su *et al*., 2024). We found significant associations between all xylem traits of mistletoes and those of their hosts, with the slopes of these trait correlations being significantly different from 1 (Fig. S4), suggesting the influence of hosts on mistletoe xylem traits. Watson (2009) proposed the 'host quality hypothesis', positing that 'quality' pertains to the ability of a host to provide water, nutrients, or other resources. For example, in this study, we found that mistletoe *Scurrula chingii* var. *yunnanensis* H.S.Kiu parasitizing a liana had a larger diameter than other pairs, suggesting anatomical plasticity in responses to the hosts. Additionally, Sibinelli & Ceccantini (2022) identified seasonal variations in cambial activity of mistletoes, which could be influenced by the seasonal phenology of the hosts. As reported by Amaral & Ceccantini (2011) and Teixeira-Costa & Ceccantini (2015), lower water potentials in hosts may alter the turgor in differentiating fusiform cells. Taken together, hosts significantly affect both the variation in mistletoe xylem traits and their responses to environmental changes. In addition, it is interesting to investigate the controlled effect of collecting height throughout the canopy of hosts on mistletoe hydraulic traits for future studies.

Conclusions

Our results clearly show that mistletoes employ a hydraulic strategy with high safety but low efficiency, contrasting with their hosts. Relatively slow water transport with high embolism resistance agrees with their high xylem tension (low water potentials), but contradicts their high transpiration and low water use efficiency. Their apparent aggressive water use could be realized by maintaining high stomatal conductance at low water potentials, which guarantees further studies. By analyzing a broad range of mistletoe–host species pairs across diverse environments with different water and temperature conditions, our study highlights the divergent ecological strategies in responding to environmental changes between mistletoes and their hosts. Compared with hosts, mistletoes showed weaker responses in hydraulic efficiency-related traits (vessel diameter, K_t) to environmental gradients. Enhanced hydraulic safety supports their parasitic lifestyle, enabling them to maintain xylem function under lower water potentials. Hosts, serving as both resource providers and biotic environments, significantly impact the xylem traits of mistletoes. The absence of relationships between WD and most vessel traits in mistletoes could be because of their small variations in traits. The distinct trait correlations in mistletoes suggest a unique hydraulic strategy, likely shaped by their specific ecological niche and evolutionary history. Amid global change and increasing droughts, this study provides valuable insights into the future performance of mistletoes and their hosts. It highlights the specific strategies that mistletoes have developed to thrive in their parasitic lifestyle and varying environmental conditions, which is crucial for predicting their responses to climate change and for effective ecosystem management.

Acknowledgements

We thank Cai-Die Jiang, Shi-Hua Qi, Jin-Hua Qi, and Qi-Cai Zhu for field assistance and laboratory experiments and Yun-Hong Tan for species identification. The Lijiang Forest Ecosystem Research Station, the Xishuangbanna Station for Tropical Rainforest Ecosystem Studies, the Ailaoshan Station for Subtropical Forest Ecosystem Studies, and the Yuanjiang Savanna Ecosystem Research Station provided the climate and soil data. We are grateful to the Center for Gardening and Horticulture and the Institutional Center for Shared Technologies and Facilities, Xishuangbanna Tropical Botanical Garden, Chinese Academy of Sciences, for providing the collection permit and the equipment for anatomical measurements, respectively. We thank three reviewers for their constructive comments, which significantly improved this manuscript. This work was supported by the National Natural Science Foundation of China (32301308, 32171507, and 31870385), the Yunnan Fundamental Research Projects (202401AT070230), and the 14th Five-Year Plan of the Xishuangbanna Tropical Botanical Garden, CAS (XTBG-1450101). Additionally, this research was also partially funded through self-financing by our institute, which needs to be acknowledged.

Competing interests

None declared.

Author contributions

Y-BZ and J-LZ conceived and designed the experiment. Y-BZ, W-HL, X-YH, YK, QW and J-LZ collected the data. Y-BZ, J-XL, DY and J-LZ analyzed the data. Y-BZ, MCS, DSE, Y-JZ and J-LZ led the writing. All authors contributed critically to the drafts and gave final approval for publication.

ORCID

Marina Corrêa Scalon https://orcid.org/0000-0003-2069-8226
David S. Ellsworth https://orcid.org/0000-0002-9699-2272
Xian-Yan Huang https://orcid.org/0009-0007-3083-1576
Yan Ke https://orcid.org/0000-0002-3579-2584
Jing-Xin Liu https://orcid.org/0000-0003-4127-7252
Qin Wang https://orcid.org/0000-0002-0521-4484
Da Yang https://orcid.org/0000-0001-7306-3289
Jiao-Lin Zhang https://orcid.org/0000-0003-3693-7965
Yong-Jiang Zhang https://orcid.org/0000-0001-5637-3015
Yun-Bing Zhang https://orcid.org/0000-0002-2739-4324

Data availability

All data supporting the findings of this study are available in Dataset S1.

References

Alvarado MV, Terrazas T. 2023. Tree species differ in plant economic spectrum traits in the tropical dry forest of Mexico. *PLoS ONE* **18**: e0293430.

Amaral MM, Ceccantini G. 2011. The endoparasite *Pilostyles ulei* (Apodanthaceae – Cucurbitales) influences wood structure in three host species of *Mimosa*. *IAWA Journal* **32**: 1–13.

Anderson MJ. 2001. A new method for non-parametric multivariate analysis of variance. *Austral Ecology* **26**: 32–46.

Anfodillo T, Carraro V, Carrer M, Fior C, Rossi S. 2006. Convergent tapering of xylem conduits in different woody species. *New Phytologist* **169**: 279–290.

Apgaua DMG, Tng DYP, Laurance SGW. 2022. Tropical wet and dry forest tree species exhibit contrasting hydraulic architecture. *Flora* **291**: 152072.

Bartoń K. 2020. *MuMIn: multi-model inference.* [WWW document] URL https://CRAN.R-project.org/package=MuMIn [accessed 22 March 2023].

Bates D, Mächler M, Bolker B, Walker S. 2015. Fitting linear mixed-effects models using LME4. *Journal of Statistical Software* **67**: 1–48.

Bell DM, Pabst RJ, Shaw DC. 2020. Tree growth declines and mortality were associated with a parasitic plant during warm and dry climatic conditions in a temperate coniferous forest ecosystem. *Global Change Biology* **26**: 1714–1724.

Carlquist S. 1977. Ecological factors in wood evolution: a floristic approach. *American Journal of Botany* **64**: 887–896.

Carlquist S. 1984. Vessel grouping in dicotyledon wood: significance and relationship to imperforate tracheary elements. *Aliso* **10**: 505–525.

Carlquist SJ. 2009. Non-random vessel distribution in woods: patterns, modes, diversity, correlations. *Aliso* **27**: 39–58.

Carvalho ECD, Souza BC, Silva MS, Menezes BS, Martins FR, Araújo FS, Soares AA. 2023. Xylem anatomical traits determine the variation in wood density and water storage of plants in tropical semiarid climate. *Flora* **298**: 152185.

Castelar JVS, Da Cunha M, Simioni PF, Castilhori MF, Lira-Martins D, Giles AL, Costa WS, Alexandrino CR, Callado CH. 2023. Functional traits and water-transport strategies of woody species in an insular environment in a tropical forest. *American Journal of Botany* **110**: e16214.

Chave J, Coomes D, Jansen S, Lewis SL, Swenson NG, Zanne AE. 2009. Towards a worldwide wood economics spectrum. *Ecology Letters* **12**: 351–366.

Chen YJ, Choat B, Sterck F, Maenpuen P, Katabuchi M, Zhang SB, Tomlinson KW, Oliveira RS, Zhang YJ, Shen JX *et al.* 2021. Hydraulic prediction of drought-induced plant dieback and top-kill depends on leaf habit and growth form. *Ecology Letters* **24**: 2350–2363.

Chen ZC, Zhu SD, Zhang YT, Luan JW, Li S, Sun PS, Wan XC, Liu SR. 2020. Tradeoff between storage capacity and embolism resistance in the xylem of temperate broadleaf tree species. *Tree Physiology* **40**: 1029–1042.

Crates R, Watson DM, Albery GF, Bonnet T, Murphy L, Rayner L, Stojanovic D, Timewell C, Meney B, Roderick M *et al.* 2022. Mistletoes could moderate drought impacts on birds, but are themselves susceptible to drought-induced dieback. *Proceedings of the Royal Society B: Biological Sciences* **289**: 20220358.

Ewers FW, Jacobsen AL, López-Portillo J. 2023. Carlquist's indices for vulnerability and mesomorphy of wood: are they relevant today? *IAWA Journal* **44**: 355–367.

Fajardo A. 2022. Wood density relates negatively to maximum plant height across major angiosperm and gymnosperm orders. *American Journal of Botany* **109**: 250–258.

Fajardo A, Martínez-Pérez C, Cervantes-Alcayde MA, Olson ME. 2020. Stem length, not climate, controls vessel diameter in two trees species across a sharp precipitation gradient. *New Phytologist* **225**: 2347–2355.

Fajardo A, Piper FI, García-Cervigón AI. 2022. The intraspecific relationship between wood density, vessel diameter and other traits across environmental gradients. *Functional Ecology* **36**: 1585–1598.

Fontes CG, Pinto-Ledezma J, Jacobsen AL, Pratt RB, Cavender-Bares J. 2022. Adaptive variation among oaks in wood anatomical properties is shaped by climate of origin and shows limited plasticity across environments. *Functional Ecology* **36**: 326–340.

Fontúrbel FE, Lara A, Lobos D, Little C. 2018. The cascade impacts of climate change could threaten key ecological interactions. *Ecosphere* **9**: e02485.

Garcia MN, Ferreira MJ, Ivanov V, dos Santos VAHF, Ceron JV, Guedes AV, Saleska SR, Oliveira RS. 2021. Importance of hydraulic strategy trade-offs in structuring response of canopy trees to extreme drought in central Amazon. *Oecologia* **197**: 13–24.

Gebauer R, Albrechtova P, Plichta R, Volarik D. 2019. The comparative xylem structure and function of petioles and twigs of mistletoe *Loranthus europaeus* and its host *Quercus pubescence*. *Trees* **33**: 933–942.

Glatzel G, Geils BW. 2009. Mistletoe ecophysiology: host-parasite interactions. *Botany* **87**: 10–15.

Gleason SM, Westoby M, Jansen S, Choat B, Hacke UG, Pratt RB, Bhaskar R, Brodribb TJ, Bucci SJ, Cao K-F *et al.* 2016. Weak tradeoff between xylem safety and xylem-specific hydraulic efficiency across the world's woody plant species. *New Phytologist* **209**: 123–136.

Goldstein G, Rada F, Sternberg L, Burguera JL, Burguera M, Orozco A, Montilla M, Zabala O, Azocar A, Canales MJ *et al.* 1989. Gas-exchange and water-balance of a mistletoe species and its mangrove hosts. *Oecologia* **78**: 176–183.

Griebel A, Peters JMR, Metzen D, Maier C, Barton CVM, Speckman HN, Boer MM, Nolan RH, Choat B, Pendall E. 2022. Tapping into the physiological responses to mistletoe infection during heat and drought stress. *Tree Physiology* **42**: 523–536.

Guérin M, von Arx G, Martin-Benito D, Andreu-Hayles L, Griffin KL, McDowell NG, Pockman W, Gentine P. 2020. Distinct xylem responses to acute vs prolonged drought in pine trees. *Tree Physiology* **40**: 605–620.

Hacke UG, Jacobsen AL, Pratt RB. 2022. Vessel diameter and vulnerability to drought-induced embolism: within-tissue and across-species patterns and the issue of survivorship bias. *IAWA Journal* **44**: 304–319.

Hacke UG, Sperry JS, Pockman WT, Davis SD, McCulloh KA. 2001. Trends in wood density and structure are linked to prevention of xylem implosion by negative pressure. *Oecologia* **126**: 457–461.

Hacke UG, Spicer R, Schreiber SG, Plavcová L. 2017. An ecophysiological and developmental perspective on variation in vessel diameter. *Plant, Cell & Environment* **40**: 831–845.

Haynes AF. 2022. What do we know about parasitic plants and the leaf economic spectrum? *Journal of Plant Ecology* **15**: 691–699.

He XF, Wang SW, Körner C, Yang Y. 2021. Water and nutrient relations of mistletoes at the drought limit of their hosting evergreen oaks in the semiarid upper Yangtze region, SW China. *Trees* **35**: 387–394.

Isasa E, Link RM, Jansen S, Tezeh FR, Kaack L, Sarmento Cabral J, Schuldt B. 2023. Addressing controversies in the xylem embolism resistance–vessel diameter relationship. *New Phytologist* **238**: 283–296.

Islam M, Rahman M, Bräuning A. 2018. Long-term hydraulic adjustment of three tropical moist forest tree species to changing climate. *Frontiers in Plant Science* **9**: 1761.

Johnson DM, Domec J-C, Carter Berry Z, Schwantes AM, McCulloh KA, Woodruff DR, Wayne Polley H, Wortemann R, Swenson JJ, Scott Mackay D *et al.* 2018. Co-occurring woody species have diverse hydraulic strategies and mortality rates during an extreme drought. *Plant, Cell & Environment* **41**: 576–588.

Jupa R, Krabičková D, Plichta R, Mayr S, Gloser V. 2021. Do angiosperm tree species adjust intervessel lateral contact in response to soil drought? *Physiologia Plantarum* **172**: 2048–2058.

Kawai K, Minagi K, Nakamura T, Saiki S-T, Yazaki K, Ishida A. 2021. Parenchyma underlies the interspecific variation of xylem hydraulics and carbon storage across 15 woody species on a subtropical Island in Japan. *Tree Physiology* **42**: 337–350.

Lens F, Gleason SM, Bortolami G, Brodersen C, Delzon S, Jansen S. 2022. Functional xylem characteristics associated with drought-induced embolism in angiosperms. *New Phytologist* **236**: 2019–2036.

Lens F, Sperry JS, Christman MA, Choat B, Rabaey D, Jansen S. 2011. Testing hypotheses that link wood anatomy to cavitation resistance and hydraulic conductivity in the genus *Acer*. *New Phytologist* **190**: 709–723.

Lenth R. 2021. *EMMEANS: estimated marginal means, aka least-squares means.* R package v.1.5.5-1. [WWW document] URL https://CRAN.R-project.org/package=emmeans.

Levionnois S, Jansen S, Wandji RT, Beauchêne J, Ziegler C, Coste S, Stahl C, Delzon S, Authier L, Heuret P. 2021. Linking drought-induced xylem embolism resistance to wood anatomical traits in Neotropical trees. *New Phytologist* **229**: 1453–1466.

Liang XY, He PC, Liu H, Zhu SD, Uyehara IK, Hou H, Wu GL, Zhang H, You ZT, Xiao YY *et al.* 2019. Precipitation has dominant influences on the variation of plant hydraulics of the native *Castanopsis fargesii* (Fagaceae) in subtropical China. *Agricultural and Forest Meteorology* **271**: 83–91.

Liang XY, Ye Q, Liu H, Brodribb TJ. 2021. Wood density predicts mortality threshold for diverse trees. *New Phytologist* **229**: 3053–3057.

Liu H, Ye Q, Gleason SM, He P, Yin D. 2021. Weak tradeoff between xylem hydraulic efficiency and safety: climatic seasonality matters. *New Phytologist* **229**: 1440–1452.

Liu YY, Chao L, Li ZG, Ma L, Hu BQ, Zhu SD, Cao KF. 2024. Water storage capacity is inversely associated with xylem embolism resistance in tropical karst tree species. *Tree Physiology* **44**: tpae017.

Lüdecke D, Ben-Shachar MS, Patil I, Waggoner P, Makowski D. 2021. PERFORMANCE: an R package for assessment, comparison and testing of statistical models. *Journal of Open Source Software* **6**: 3139.

Méndez-Alonzo R, Paz H, Zuluaga RC, Rosell JA, Olson ME. 2012. Coordinated evolution of leaf and stem economics in tropical dry forest trees. *Ecology* **93**: 2397–2406.

Meunier F, Krishna Moorthy SM, De Deurwaerder HPT, Kreus R, Van den Bulcke J, Lehnebach R, Verbeeck H. 2020. Within-site variability of liana wood anatomical traits: a case study in Laussat, French Guiana. *Forests* **11**: 523.

Mrad A, Johnson DM, Love DM, Domec J-C. 2021. The roles of conduit redundancy and connectivity in xylem hydraulic functions. *New Phytologist* **231**: 996–1007.

Nakagawa S, Schielzeth H. 2013. A general and simple method for obtaining R^2 from generalized linear mixed-effects models. *Methods in Ecology and Evolution* **4**: 133–142.

Oksanen J, Blanchet FG, Kindt R, Legendre P, O'Hara RB, Simpson GL, Solymos P, Stevens H, Wagner H. 2013. *VEGAN: community ecology package.* [WWW document] URL https://cran.r-project.org/web/packages/vegan/index.html.

Olson M, Rosell JA, Martínez-Pérez C, León-Gómez C, Fajardo A, Isnard S, Cervantes-Alcayde MA, Echeverría A, Figueroa-Abundiz VA, Segovia-Rivas A *et al.* 2020. Xylem vessel-diameter–shoot-length scaling: ecological significance of porosity types and other traits. *Ecological Monographs* **90**: e01410.

Olson ME, Anfodillo T, Rosell JA, Petit G, Crivellaro A, Isnard S, León-Gómez C, Alvarado-Cárdenas LO, Castorena M. 2014. Universal hydraulics of the flowering plants: vessel diameter scales with stem length across angiosperm lineages, habits and climates. *Ecology Letters* **17**: 988–997.

Olson ME, Soriano D, Rosell JA, Anfodillo T, Donoghue MJ, Edwards EJ, León-Gómez C, Dawson T, Camarero Martínez JJ, Castorena M *et al.* 2018. Plant height and hydraulic vulnerability to drought and cold. *Proceedings of the National Academy of Sciences, USA* **115**: 7551–7556.

Ozturk M, Coskuner KA, Usta Y, Serdar B, Bilgili E. 2019. The effect of mistletoe (*Viscum album*) on branch wood and needle anatomy of Scots pine (*Punts sylvestris*). *IAWA Journal* **40**: 352–365.

Pfautsch S, Harbusch M, Wesolowski A, Smith R, Macfarlane C, Tjoelker MG, Reich PB, Adams MA. 2016. Climate determines vascular traits in the ecologically diverse genus *Eucalyptus*. *Ecology Letters* **19**: 240–248.

Poorter L, McDonald I, Alarcón A, Fichtler E, Licona J-C, Peña-Claros M, Sterck F, Villegas Z, Sass-Klaassen U. 2010. The importance of wood traits and hydraulic conductance for the performance and life history strategies of 42 rainforest tree species. *New Phytologist* **185**: 481–492.

R Core Team. 2022. *R: A language and environment for statistical computing, v.4.3.2*. Vienna, Austria: R Foundation for Statistical Computing. [WWW document] URL https://www.R-project.org.

Richards JH, Henn JJ, Sorenson QM, Adams MA, Smith DD, McCulloh KA, Givnish TJ. 2021. Mistletoes and their eucalypt hosts differ in the response of leaf functional traits to climatic moisture supply. *Oecologia* **195**: 759–771.

Scalon MC, Wright IJ. 2015. A global analysis of water and nitrogen relationships between mistletoes and their hosts: broad-scale tests of old and enduring hypotheses. *Functional Ecology* **29**: 1114–1124.

Scholz A, Klepsch M, Karimi Z, Jansen S. 2013. How to quantify conduits in wood? *Frontiers in Plant Science* **4**: 56.

Shen H, Zhang J, Peng L, Tao Y, Zang YX, Li YG, Zhang YM. 2023. Spatial patterns and climatic factors influence the branch xylem anatomical traits of *Reaumuria soongarica* in the desert region of northwestern China. *Environmental and Experimental Botany* **210**: 105338.

Sibinelli V, Ceccantini G. 2022. Axial and radial wood maturation in three mistletoe 'giants' (Loranthaceae). *IAWA Journal* **43**: 1–19.

Su GF, Chen J, Zhang L. 2024. The associational effects of host plant and mistletoe functional traits on leaf herbivory in mistletoe. *Oecologia* **204**: 213–225.

Teixeira-Costa L, Ceccantini G. 2015. Embolism increase and anatomical modifications caused by a parasitic plant: *Phoradendron crassifolium* (Santalaceae) on *Tapirira guianensis* (Anacardiaceae). *IAWA Journal* **36**: 138–151.

Teixeira-Costa L, Ceccantini GCT. 2016. Aligning microtomography analysis with traditional anatomy for a 3D understanding of the host-parasite interface – *Phoradendron* spp. case study. *Frontiers in Plant Science* **7**: 1340.

Teixeira-Costa L, Heberling JM, Wilson CA, Davis CC. 2023. Parasitic flowering plant collections embody the extended specimen. *Methods in Ecology and Evolution* **14**: 319–331.

Tng DYP, Apgaua DMG, Ishida YF, Mencuccini M, Lloyd J, Laurance WF, Laurance SGW. 2018. Rainforest trees respond to drought by modifying their hydraulic architecture. *Ecology and Evolution* **8**: 12479–12491.

Tyree MT, Zimmermann MH. 2002. *Xylem structure and the ascent of sap.* Berlin, Germany: Springer.

Warton DI, Duursma RA, Falster DS, Taskinen S. 2012. smatr 3– an R package for estimation and inference about allometric lines. *Methods in Ecology and Evolution* **3**: 257–259.

Watson DM. 2009. Determinants of parasitic plant distribution: the role of host quality. *Botany* **87**: 16–21.

Watson DM, Herring M. 2012. Mistletoe as a keystone resource: an experimental test. *Proceedings of the Royal Society B: Biological Sciences* **279**: 3853–3860.

Watson DM, McLellan RC, Fontúrbel FE. 2022. Functional roles of parasitic plants in a warming world. *Annual Review of Ecology, Evolution, and Systematics* **53**: 25–45.

Wright IJ, Ackerly DD, Bongers F, Harms KE, Ibarra-Manriquez G, Martinez-Ramos M, Mazer SJ, Muller-Landau HC, Paz H, Pitman NCA *et al.* 2007. Relationships among ecologically important dimensions of plant trait variation in seven neotropical forests. *Annals of Botany* **99**: 1003–1015.

Yang D, Goldstein G, Wang M, Zhang WW, Wang AY, Liu YY, Hao GY. 2017. Microenvironment in the canopy rivals the host tree water status in controlling sap flow of a mistletoe species. *Tree Physiology* **37**: 501–510.

Yang D, Wang YSD, Wang Q, Ke Y, Zhang YB, Zhang SB, Zhang YJ, McDowell NG, Zhang JL. 2023. Physiological response and photosynthetic recovery to an extreme drought: evidence from plants in a dry-hot valley savanna of Southwest China. *Science of the Total Environment* **868**: 161711.

Ye HY, Zhao WL, Li YQ, Chen X, Zhang YX, Zhao P. 2021. Different effects of hemi-parasite *Taxillus chinensis* on water transport of its host angiosperms and gymnosperms trees. *Flora* **285**: 151955.

Zanne AE, Tank DC, Cornwell WK, Eastman JM, Smith SA, FitzJohn RG, McGlinn DJ, O'Meara BC, Moles AT, Reich PB *et al.* 2014. Three keys to the radiation of angiosperms into freezing environments. *Nature* **506**: 89–92.

Zhang L, Chen Y, Ma K, Bongers F, Sterck FJ. 2019. Fully exposed canopy tree and liana branches in a tropical forest differ in mechanical traits but are similar in hydraulic traits. *Tree Physiology* **39**: 1713–1724.

Zhang Y, Liu JB, Zhang XX. 2022. A more drought resistant stem xylem of southern highbush than rabbiteye blueberry is linked to its anatomy. *Agronomy* **12**: 1244.

Zhang YB, Corrêa Scalon M, Liu JX, Song XY, Yang D, Zhang YJ, Ellsworth DS, Zhang JL. 2023. You are what you eat: nutrient and water relations between mistletoes and hosts. *New Phytologist* **238**: 567–583.

Zhang YB, Yang D, Zhang KY, Bai XL, Wang YSD, Wu HD, Ding LZ, Zhang YJ, Zhang JL. 2022. Higher water and nutrient use efficiencies in savanna than in rainforest lianas result in no difference in photosynthesis. *Tree Physiology* **42**: 145–159.

Zhu SD, Song JJ, Li RH, Ye Q. 2013. Plant hydraulics and photosynthesis of 34 woody species from different successional stages of subtropical forests. *Plant, Cell & Environment* **36**: 879–891.

Zweifel R, Bangerter S, Rigling A, Sterck FJ. 2012. Pine and mistletoes: how to live with a leak in the water flow and storage system? *Journal of Experimental Botany* **63**: 2565–2578.

Supporting Information

Additional Supporting Information may be found online in the Supporting Information section at the end of the article.

Dataset S1 Dataset of the present study.

Fig. S1 The coefficient of variation for each xylem trait in mistletoe and host.

Fig. S2 Principal component analysis for 12 xylem traits from mistletoe–host species pairs in each site.

Fig. S3 The Pearson correlations among 12 functional traits in mistletoes and hosts, and between mistletoes and hosts.

Fig. S4 The correlations between mistletoe and host xylem traits.

Table S1 The detailed sampling results.

Table S2 Mistletoe–host (M-H) species pairs, host leaf habits, and numbers of M-H individual pairs used for measurements of xylem traits.

Table S3 The results of simple linear model and linear mixed-effects models, with species pairs and species as random effects, and each of 12 branch xylem traits of all species as response variable.

Table S4 The pairwise contrast of 12 xylem traits between mistletoes and hosts among four sites based on the linear mixed-effects model results.

Table S5 Effects of life form and aridity index on the xylem traits analyzed using linear mixed-effects model.

Table S6 Loadings of 12 functional traits on the first four principal components for mistletoe–host species pairs among four sites.

Table S7 PERMANOVA on the Euclidean distance of 12 xylem traits for mistletoe–host species pair mean values in each site.

Table S8 Tests of the slope, intercept, and shift for bivariate relationships between different life forms using standardized major axis regression analyses.

Table S9 PERMANOVA on the Euclidean distance of 12 xylem traits for each life form among four sites.

Table S10 Loadings of 12 functional traits on the first four principal components for host species across four sites.

Table S11 Loadings of 12 functional traits on the first four principal components for mistletoe species across four sites.